the FEBS Journal

Functional analysis of a murine monoclonal antibody against the repetitive region of the fibronectin-binding adhesins fibronectin-binding protein A and fibronectin-binding protein B from *Staphylococcus aureus*

Giulio Provenza[1,*], Maria Provenzano[1,*], Livia Visai[1,2], Fiona M. Burke[3], Joan A. Geoghegan[3], Matteo Stravalaci[4], Marco Gobbi[4], Giuliano Mazzini[5], Carla Renata Arciola[6], Timothy J. Foster[3] and Pietro Speziale[1]

1 Department of Biochemistry, University of Pavia, Italy
2 Center for Tissue Engineering (CIT), University of Pavia, Italy
3 Department of Microbiology, Moyne Institute of Preventive Medicine, University of Dublin, Ireland
4 Department of Biochemistry and Molecular Pharmacology, Istituto di Ricerche Farmacologiche 'Mario Negri', Milan, Italy
5 IGM-CNR Histochemistry & Cytometry, Department of Animal Biology, University of Pavia, Italy
6 Research Unit on Implant Infections, Rizzoli Orthopedic Institute, Bologna, Italy

Keywords
adhesin; antibody; fibronectin; repeat; *Staphylococcus*

Correspondence
P. Speziale, University of Pavia, Department of Biochemistry, Viale Taramelli 3/b, 27100 Pavia, Italy
Fax: +39 0382 423108
Tel: +39 0382 987787
E-mail: pspeziale@unipv.it

*These authors contributed equally to this work

(Received 17 June 2010, revised 22 July 2010, accepted 25 August 2010)

doi:10.1111/j.1742-4658.2010.07835.x

Fibronectin-binding proteins A and B are multifunctional LPXTG staphylococcal adhesins, comprising an N-terminal region that binds fibrinogen and elastin, and a C-terminal domain that interacts with fibronectin. The C-terminal domain of fibronectin-binding protein A is organized into 11 tandem repeats, six of which bind the ligand with high affinity; other sites bind more weakly. Fibronectin-binding protein B has been postulated to harbor 10 rather than 11 repeats, but it contains the same number of high-affinity fibronectin-binding sites as fibronectin-binding protein A. In this study, we confirm this prediction and show that six of 10 sites bind with dissociation constants in the nanomolar range. We also found that the full-length repetitive region of fibronectin-binding protein B stimulated the production of a mAb (15E11) that binds with high affinity to an epitope shared by repeats 9 and 10 from both adhesins. With the use of truncated fragments of repeat 9 of fibronectin-binding protein A, we mapped the antibody epitope to the N-terminal segment and the fibronectin-binding site to the C-terminal segment of the repeat. The distinct localization of the 15E11 epitope and the fibronectin-binding site suggests that the interfering effect of the antibody might result from steric hindrance or a conformational change in the structure that reduces the accessibility of fibronectin to its binding determinant. The epitope is well exposed on the surface of staphylococcal cells, as determined by genetic analyses, fluorescence microscopy, and flow cytometry. When incubated with cells of *Staphylococcs aureus* strains, 15E11 inhibits attachment of bacteria to surface-coated fibronectin by almost 70%.

Abbreviations
FITC, fluorescein isothiocyanate; Fn, fibronectin; FnBPA, fibronectin-binding protein A; FnBPB, fibronectin-binding protein B; FnBR, fibronectin-binding repeat; FnBRA, fibronectin-binding repeat region of FnBPA; FnBRB, fibronectin-binding repeat region of FnBPB; GST, glutathione *S*-transferase; HRP, horseradish peroxidase; LIBS, ligand-induced binding site; MSCRAMM, microbial surface components recognizing adhesive matrix molecule; NTD, N-terminal domain; RU, resonance units; SPR, surface plasmon resonance.

Structured digital abstract:

- MINT-7991189, MINT-7991227, MINT-7991305, MINT-7991292, MINT-7991279, MINT-7991266, MINT-7991253, MINT-7991622: *fnbA* (uniprotkb:P14738) *binds* (MI:0407) to *Fibronectin* (uniprotkb:P02751) by *enzyme linked immunosorbent assay* (MI:0411)
- MINT-7991435, MINT-7991636, MINT-7991447, MINT-7991462, MINT-7991477, MINT-7991492, MINT-7991507, MINT-7991522: *fnbA* (uniprotkb:P14738) *binds* (MI:0407) to *Fibronectin* (uniprotkb:P02751) by *filter binding* (MI:0049)
- MINT-7991577, MINT-7991594: *fnbB* (uniprotkb:Q53682) *binds* (MI:0407) to *Fibronectin* (uniprotkb:P02751) by *surface plasmon resonance* (MI:0107)
- MINT-7991321, MINT-7991345, MINT-7991360, MINT-7991375, MINT-7991390, MINT-7991405, MINT-7991420: *fnbB* (uniprotkb:Q53682) *binds* (MI:0407) to *Fibronectin* (uniprotkb:P02751) by *filter binding* (MI:0049)
- MINT-7991103, MINT-7991114, MINT-7991126, MINT-7991138, MINT-7991153, MINT-7991165, MINT-7991177: *fnbB* (uniprotkb:Q53682) *binds* (MI:0407) to *Fibronectin* (uniprotkb:P02751) by *enzyme linked immunosorbent assay* (MI:0411)
- MINT-7991540, MINT-7991558: *fnbA* (uniprotkb:P14738) *binds* (MI:0407) to *Fibronectin* (uniprotkb:P02751) by *surface plasmon resonance* (MI:0107)

Introduction

Staphylococcus aureus, one of the most important Gram-positive pathogens of humans and animals, is a highly versatile bacterium capable of causing a wide spectrum of diseases, ranging from superficial skin infections [1,2] to life-threatening diseases such as septic arthritis, pneumonia, septicemia, and endocarditis [3–7]. It is also a major cause of infections associated with indwelling medical devices, such as prostheses and catheters [8]. The increased virulence and resistance to antibiotics exhibited by this bacterium make the understanding of its pathogenic mechanisms an urgent challenge [9,10]. *S. aureus* produces a variety of cell surface-associated and extracellular factors that enable bacteria to colonize and multiply within the host to evade host defences and to destroy host tissues [11]. Attachment to host tissue is considered to be a critical early step in the infection process. A family of cell surface adhesins termed 'microbial surface components recognizing adhesive matrix molecules' (MSCRAMMs) bind to extracellular matrix proteins, such as fibronectin (Fn), and use these as a bridge between the bacterial surface and host cell receptors [12].

S. aureus MSCRAMMs that bind to collagen, Fn and fibrinogen have been identified and characterized in detail [12].

Fn is a large glycoprotein present in a soluble form in body fluids and in an insoluble, fibrillar form in the extracellular matrix. Its main functions include cell adhesion and spreading, regulation of cell shape and migration, and differentiation of many cell types [13]. Fn is a dimer of two similar polypeptides held together by a pair of disulfide bonds at their C-termini. It is one of the main proteins deposited on implanted biomaterials [14]. The protein has a modular structure and is composed of type 1, type 2 and type 3 (F1, F2, and F3) modules. The bacterial binding site in the N-terminal domain (NTD) of Fn contains five sequential F1 modules [15–18]. *S. aureus* expresses a number of proteins that can bind specifically to Fn [19,20]. The prototype of this class of protein is Fn-binding protein A (FnBPA) [21]. The structural characteristics of FnBPA include a C-terminal hydrophobic tail, an LPXTG motif that is critical for attachment to the cell wall, and a disordered region with Fn-binding activity. FnBPA also possesses fibrinogen-binding [22] and tropoelastin-binding abilities, mediated by the N-terminal A-domain region [23].

The Fn-binding moiety is organized into 11 tandem repeats, each interacting with the NTD of Fn. Six of these repeats bind the NTD with dissociation constants in the nanomolar range [21]. It has been proposed that each FnBPA repeat binds a string of three or four F1 modules in the NTD through a variation of the tandem β-zipper mechanism, which was discovered in *Streptococcus agalactiae* interactions with ^{1}F1^{2}F1 [24]. The crystal structure of Fn-binding sites from FnBPA in complex with Fn domains has been reported [25]. *S. aureus* contains a second Fn-binding protein, termed Fn-binding protein B (FnBPB), which shows very significant sequence homology (68%) and has an organization and function similar to those of FnBPA [26]. In fact, as is the case for FnBPA, the N-terminal region of FnBPB interacts with fibrinogen and elastin [23], whereas the C-terminal repetitive region binds Fn [26]. On the basis of sequence alignment, it has been predicted that FnBPB contains 10 rather than 11 repeats [21] (Fig. 1). Clinical isolates contain at least one *fnb* gene, and many contain two [27,28]. Both Fn-binding proteins participate in chronic staphylococcal infection by promoting adhesion to surgical implants [29].

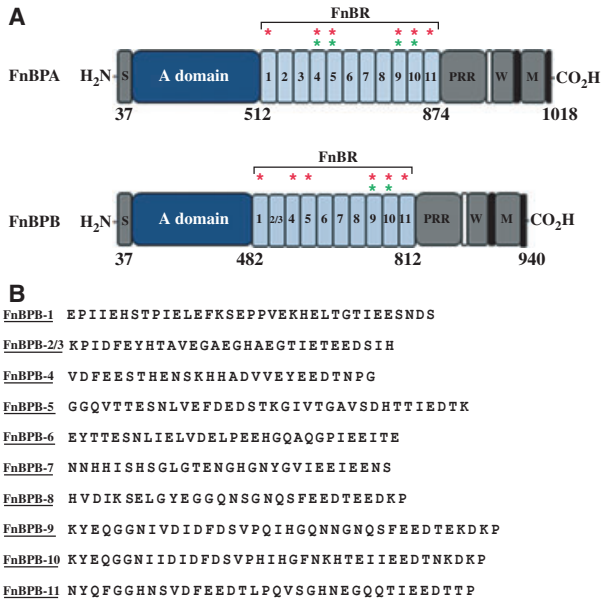

Fig. 1. Structural organization of FnBPA and FnBPB of *S. aureus* strain 8325-4. (A) The locations of the secretory signal sequence (S), fibrinogen/elastin-binding region A, the predicted FnBRs (11 and 10 repeats in FnBPA and FnBPB, respectively), the proline-rich repeats (PRR), the cell wall-spanning sequence (W) and the membrane-spanning region (M) in each protein are indicated. Binding repeats with high affinity for Fn and 15E11 are indicated by red and green asterisks, respectively. It is of note that the high-affinity Fn-binding sites in FnBPA are retained in FnBPB. (B) The amino acid sequences of the 10 FnBRs of FnBPB (Swiss-Prot entry Q53682).

The interaction between Fn-binding proteins and integrin $\alpha_5\beta_1$ on fibroblasts [30], epithelial cells [31,32] and endothelial cells [32,33] is critical in promoting *S. aureus* colonization and invasion. Deletion of the Fn-binding proteins from *S. aureus* is associated with a poorly adhesive, noninvasive phenotype [31]. It is believed that the ability of *S. aureus* to invade the host cells is important for causing chronic infection, because the bacterium can protect itself from antibiotics and host defences. Upon interaction with endothelial cells, Fn-binding proteins induce proinflammatory responses, including expression of cell adhesion molecules and secretion of chemokines and cytokines [34]. Fn-binding proteins also mediate activation of human platelets via fibrinogen and Fn bridges to integrin GpIIb/IIIa [35].

The goal of this study was to identify and characterize immunologically the main Fn-binding sites in FnBPB. In particular, we demonstrate, as previously reported for FnBPA, that Fn binds to particular repeats, and we report measurements of the affinities. We also show that the high-affinity binding sites in FnBPB correspond to those discovered in the repetitive region of FnBPA. Finally, we selected and characterized a mAb produced against the recombinant repetitive region of FnBPB that recognizes an epitope shared by repeats of FnBPA and FnBPB, and inhibits staphylococcal attachment to Fn. Taken together, these data strongly suggest the conservation of structural and functional features of the Fn-binding moieties of FnBPA and FnBPB.

Results

High-affinity binding sites for full-length Fn and its N-terminal fragment in FnBPA and FnBPB

In a previous study, detailed characterization of the biochemical and immunological properties of the FnBPA repeat region was reported [21]. Here, we have extended the analysis to FnBPB. We constructed recombinant clones expressing single Fn-binding repeats (FnBRs) of FnBPA and FnBPB fused to glutathione *S*-transferase (GST). The purity of the isolated recombinant FnBPB and FnBPA repeats was verified by SDS/PAGE (Fig. S1). Figure 2A,C shows the results of an ELISA binding assay in which the reactivities of the FnBRs from FnBPA and FnBPB for intact Fn were compared. We identified six potential high-affinity Fn-binding motifs (FnBPB-1, FnBPB-4, FnBPB-5, FnBPB-9, FnBPB-10, and FnBPB-11) in both proteins, and low-affinity binding sites in the remaining motifs. This was confirmed when the single repeats were subjected to SDS/PAGE and then tested with an Fn blotting assay (Fig. 1B,D). The similarity of the results obtained when either FnBPA or FnBPB repeats were used in the assays confirms the almost identical organization of the repeat regions in both proteins. Dose–response binding experiments in an ELISA format showed that Fn bound to FnBPB repeats in a saturable manner, and confirmed that FnBPB-1, FnBPB-5 and FnBPB-9 bound to Fn with higher affinity than FnBPB-2/3 and FnBPB-6 (data not shown).

BIAcore experiments were performed in which the GST–FnBRs were bound to a chip, and increasing concentrations of NTD were passed over the chip. These showed that motifs 9 and 10 of both adhesins interacted with the NTD, with dissociation constants (K_D) in the nanomolar range at physiological ionic strength (Fig. 3). From analysis of the equilibrium binding data, the dissociation constants for interaction with the NTD were as follows: FnBPA-9, 17.8 ± 1.1 nM; FnBPA-10, 41.8 ± 8.4 nM; FnBPB-9, 68.0 ± 21 nM; and FnBPB-10, 103.2 ± 35 nM. This indicates that the NTD binds to GST–FnBRs with similar affinities (Table 1).

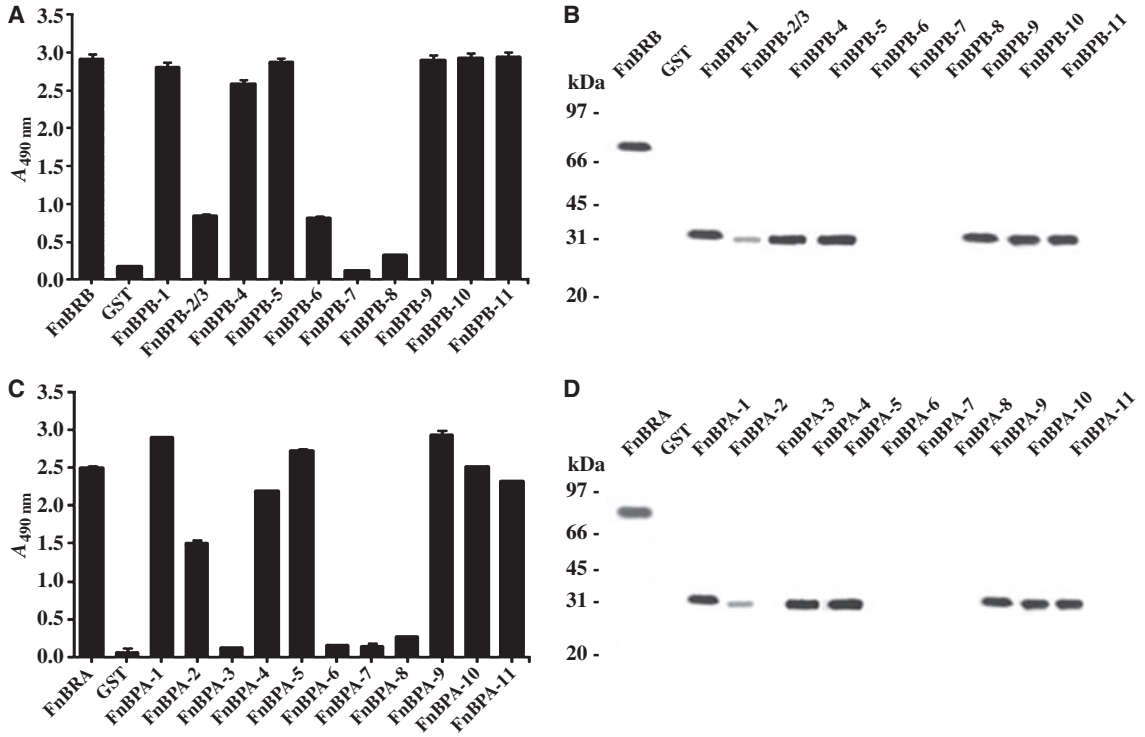

Fig. 2. Binding of Fn to the predicted FnBRs of FnBPB and FnBPA. (A, C) ELISA. Recombinant His-tagged FnBRB (A) and FnBRA (C) and their FnBRs in fusion with GST were immobilized on microtiter wells (1 μg in 100 μL) and probed with 100 μL of 10 μg·mL^{-1} Fn. After washing, the wells were incubated with 2 μg of a rabbit polyclonal antibody against Fn. Bound antibody was detected by incubation with secondary antibody [HRP-conjugated goat anti-(rabbit IgG)]. (B, D) Western blot. Purified amounts (8 μg) of FnBRB (B), FnBRA (D) and their single repeats were separated on a 12.5% polyacrylamide gel under nonreducing conditions, and then electroblotted onto nitrocellulose membranes. The membranes were incubated with 10 μg of Fn and, after washing, bound Fn was visualized by incubation with rabbit polyclonal antibody against Fn followed by addition of peroxidase-conjugated goat anti-(rabbit IgG).

Monoclonal antibodies against FnBRs of FnBPB

A panel of mouse mAbs was produced against the recombinant repetitive region of FnBPB. Analysis of mAbs binding to the recombinant FnBR indicated the generation of two categories of antibody. One group bound marginally to the purified full-length FnBR region of FnBPB (FnBRB), even after prolonged incubation, whereas a second group of mAbs interacted with high reactivity (data not shown). When the first group of antibodies was tested in the presence of soluble Fn, their reactivity with FnBRB was significantly stronger than in the absence of the ligand. Thus, it appears that FnBRB possesses ligand-induced binding site (LIBS) epitopes, i.e. determinants exposed upon binding of the ligand (Fn) (manuscript in preparation). The second group of mAbs against FnBRB included antibodies that bound the antigen in the absence of Fn. One of these mAbs, designated 15E11, was selected for further study.

15E11 is a mAb that recognizes an epitope shared by distinct FnBPA/FnBPB repeats

Mapping the 15E11 epitopes

In an attempt to map the epitopes recognized by 15E11, the collection of Fn-binding single repeats of FnBPB fused to GST were examined by ELISA. As shown in Fig. 4A, the antibody recognized FnBPB-9 and FnBPB-10. These results were confirmed in immunoblotting experiments by incubating the individual FnBRs on a nitrocellulose membrane with 15E11 (Fig. 4B). When the FnBRs of FnBPA were tested with 15E11 in ELISA and by western immunoblotting, FnBPA-9 and FnBPA-10 showed reactivities similar to those exhibited by the homologous repeats of FnBPB. Additionally, the ELISA assay and western immunoblotting revealed weak recognition of FnBPA-4 and FnBPA5 by 15E11 (Fig. 4C,D).

To confirm the localization of the epitope, we constructed a truncated form of FnBRB from which

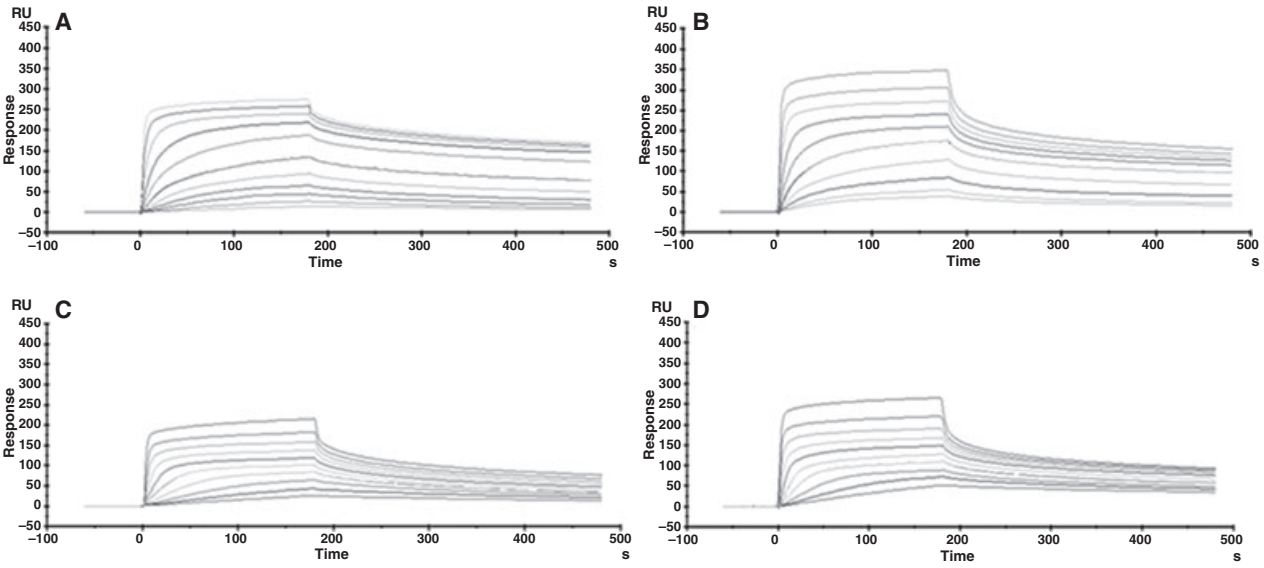

Fig. 3. SPR analysis of NTD binding to FnBRs of FnBPA and FnBPB fused to GST. Different concentrations of the NTD were compared for binding to GST–repeats immobilized on the surface of a CM5 sensor chip. Sensorgrams of the binding to GST–repeats were obtained by passing increasing concentrations of the NTD (0.5–512 nM) over FnBPA-9 (A), FnBPA-10 (B), FnBPB-9 (C), and FnBPB-10 (D) (2–1024 nM). Injection began at 0 s and ended at 180 s.

Table 1. Affinity parameters for NTD–FnBR interactions. The parameters were determined by SPR measurements, with immobilized FnBRs of FnBPA and FnBPB as ligands and the NTD as the analyte. K_D, dissociation equilibrium constant.

Protein	K_D (nM)
FnBPA-9	17.8 ± 1.1
FnBPA-10	41.8 ± 8.4
FnBPB-9	68.0 ± 21
FnBPB-10	103.2 ± 35

the contiguous repeats 9 and 10 were deleted (FnBRBΔ9,10). The protein was then tested for binding to Fn by ELISA and western immunoblotting (Fig. 5). Whereas significant binding of FnBRBΔ9,10 to Fn was conserved (Fig. 5A,B), the reactivity of 15E11 with FnBRBΔ9,10 was completely abolished (Fig. 5C,D).

The reactivity of 15E11 with FnBRA and FnBRAΔ9,10 was also tested. As shown in Fig. 6A,B, deletion of repeats 9 and 10 did not affect the interaction of FnBRBΔ9,10 with Fn. In contrast, a significant reduction in antibody binding was observed by ELISA and western immunoblotting when 15E11 was incubated with FnBRAΔ9,10 as compared with the binding of 15E11 to the intact repeat region (Fig. 6C,D). The residual binding of 15E11 to FnBRAΔ9,10 could be a consequence of the weak binding of repeats 4 and 5 to the antibody.

15E11 affinity for the relevant epitopes

The affinity of 15E11 for its epitopes was determined by surface plasmon resonance (SPR). The antibody was covalently immobilized on a chip by using amine-coupling chemistry, and this was followed by the injection of soluble repeats 9 or 10 of both FnBPA and FnBPB across the sensor chip surface. Table 2 reports the kinetic constants of the binding and the calculated K_D values. The affinities of 15E11 for the repeats ranged from 40–45 nM (FnBPA repeats) to 140–200 nM (FnBPB repeats).

Further definition of the 15E11 epitope in FnBPA-9

On the basis of the above findings (Table 2), FnBPA-9 represents the repeat with the highest affinity for 15E11. Thus, it was hypothesized that the FnBPA-9 repeat harbors a more discrete binding site that is capable of interacting with 15E11. To validate this assumption, we constructed subfragments of FnBPA-9 by removing the first 10 N-terminal or the last 10 C-terminal amino acids (Fig. 7A). Loss of N-terminal amino acids 1–10 of FnBPA-9 almost completely eliminated 15E11-binding activity, suggesting that this region carries amino acids that are essential for 15E11 binding, or that it indirectly participates in the formation of or stabilization of the epitope (Fig. 7B,D). In contrast, the truncated form lacking the extreme C-terminal segment

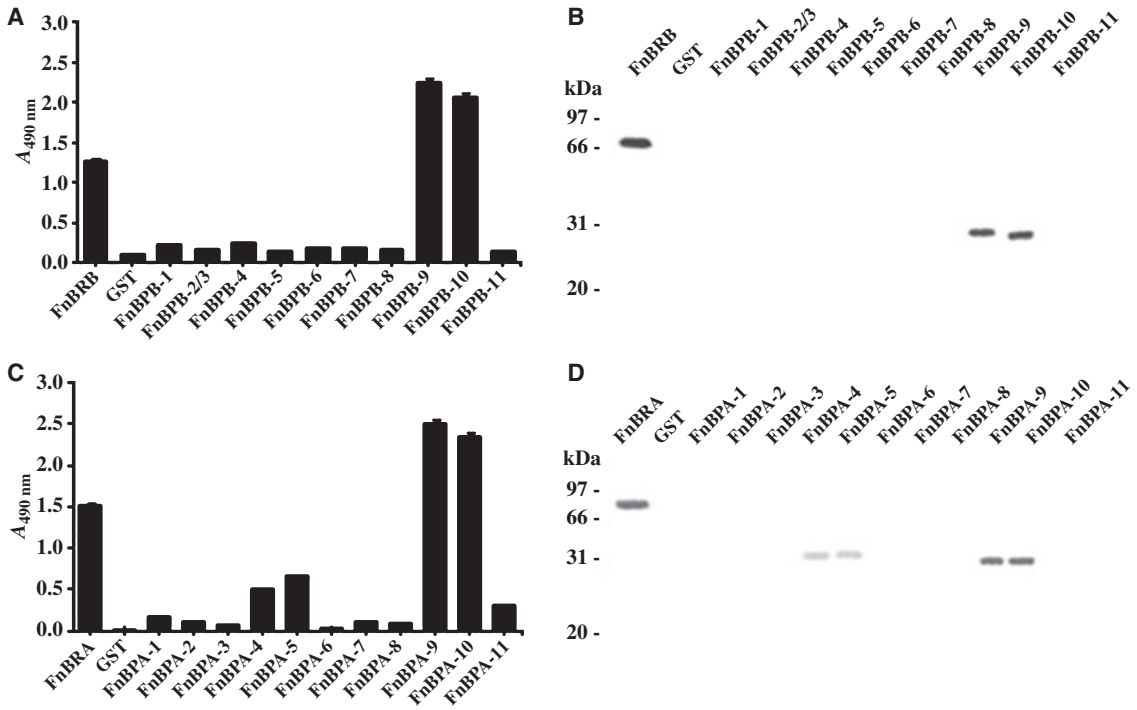

Fig. 4. Binding of 15E11 to the predicted FnBRs of FnBPB and FnBPA. (A, C) ELISA. Recombinant His-tagged FnBRB (A) and FnBRA (C) and their FnBRs in fusion with GST were immobilized on microtiter wells (1 μg in 100 μL) and probed with 100 μL of 10 $\mu g \cdot mL^{-1}$ 15E11. Bound antibody was detected by incubating with secondary antibody [HRP-conjugated rabbit anti-(mouse IgG)]. (B, D) Western blot. Purified amounts (8 μg) of FnBRB (B), FnBRA (D) and their single repeats were separated on 12.5% polyacrylamide gel and electroblotted onto nitrocellulose membranes. The membranes were incubated with 10 μg of 15E11. Bound antibody was visualized with HRP-conjugated rabbit anti-(mouse IgG).

(amino acids 29–38) lost Fn-binding activity but not 15E11-binding ability. Thus, Fn and 15E11 recognize different regions of FnBPA-9 (Fig. 7C,E).

Epitopes of 15E11 are displayed on the surface of *S. aureus* strains

To determine whether the epitopes recognized by 15E11 are displayed on the staphylococcal cell surface, a genetic approach was used in which mutants of *S. aureus* strains SH1000 and P1 lacking protein A and Fn-binding proteins were complemented with plasmid pCU1 carrying the full-length *fnbA* gene or *fnbAΔ 9,10*. Adhesion to immobilized elastin and Fn was measured, as well as binding of 15E11. As shown in Fig. 8A,B,D,E, adherence of the complemented strains to either elastin or Fn did not differ substantially from that of the wild-type strains, suggesting that the entire FnBPA protein was expressed. Furthermore, bacteria expressing FnBPA bound 15E11 strongly, whereas the strain expressing FnBPAΔ9,10 showed a significant reduction ($P < 0.05$) (Fig. 8C,F). Taken together, these data demonstrate that repeats 9 and 10 of FnBPA are fully exposed on the surface of staphylococcal cells and are recognized by 15E11.

Immunofluorescent staining of *S. aureus* strains SH1000, P1 and Cowan 1 from which the gene for protein A (*spa*) was deleted confirmed the surface localization of the epitopes. Bright fluorescent staining was observed with cells incubated with 15E11, but not with those incubated with an unrelated mAb (14G6), confirming that the epitopes in repeats 9 or 10 of FnBPA and FnBPB are exposed on the cell surface (data not shown). Furthermore, the fluorescein isothiocyanate (FITC)-labeled antibody demonstrated significant surface binding to the staphylococcal strains as compared with the control mAb 14G6 when evaluated by flow cytometry (data not shown).

15E11 affects attachment of *S. aureus* strains to surface-coated Fn

To determine whether 15E11 could inhibit adherence of staphylococci to immobilized Fn, strains SH1000 *spa*, Cowan 1 *spa* or P1 *spa* and the clinical isolate MRSA190 were incubated with increasing concentrations

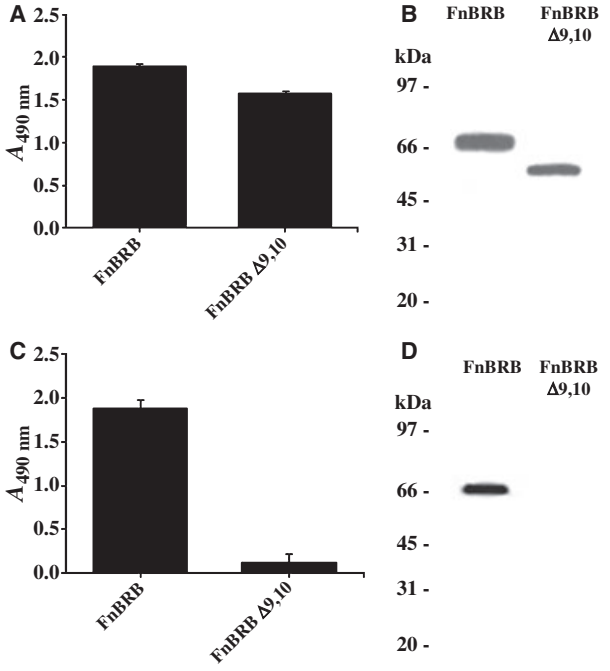

Fig. 5. Binding of Fn or 15E11 to FnBRB lacking FnBPB-9 and FnBPB-10. (A, C) ELISA. Recombinant His-tagged entire FnBRB and FnBRB lacking FnBPB-9 and FnBPB-10 were immobilized on microtiter wells (1 μg in 100 μL) and probed with 100 μL of 10 μg·mL^{-1} Fn (A) or with 100 μL of 10 μg·mL^{-1} 15E11 (C). After washing, Fn-bound wells (A) were incubated with 2 μg of rabbit polyclonal antibody against Fn. Binding of the polyclonal antibody (A) or mAb (B) was detected by incubating the wells with HRP-conjugated goat anti-(rabbit IgG) or secondary antibody [HRP-conjugated rabbit anti-(mouse IgG)], respectively. (B, D) Western blot. Purified amounts (8 μg) of entire FnBRB and FnBRB lacking FnBPB-9 and FnBPB-10 were separated on a 12.5% polyacrylamide gel and then electroblotted onto nitrocellulose membranes. The membranes were incubated with 10 μg of Fn (B) or 10 μg of 15E11 (D). Membranes incubated with Fn were washed and further incubated with rabbit polyclonal antibody against Fn. Binding of the polyclonal antibody (B) or mAb (D) to the filters was visualized by addition of HRP-conjugated goat anti-(rabbit IgG) or rabbit anti-(mouse IgG), respectively.

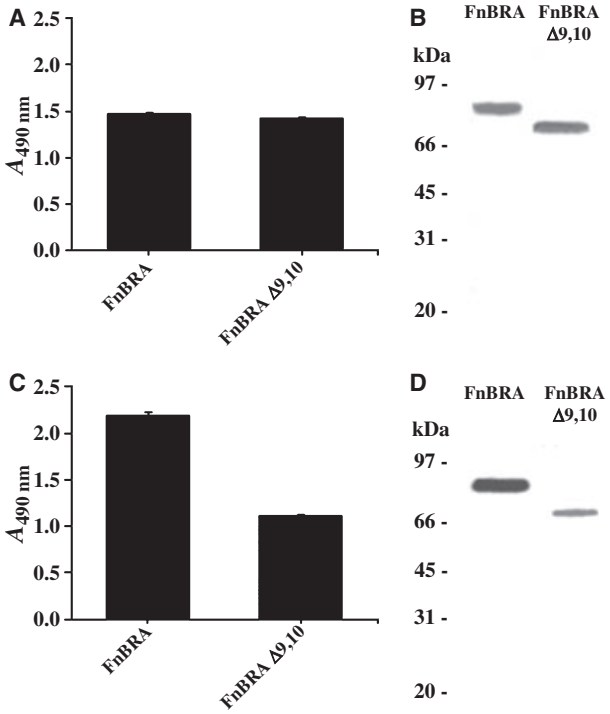

Fig. 6. Binding of Fn or 15E11 to FnBRA lacking FnBPA-9 and FnBPA-10. (A, C) Recombinant, His-tagged full-length FnBRA and FnBRA lacking FnBPA-9 and FnBPA-10 (FnBRAΔ9,10) were immobilized on microtiter wells (1 μg in 100 μL) and probed with 100 μL of 10 μg·mL^{-1} Fn (A) or 100 μL of 10 μg·mL^{-1} 15E11 (C). After washing, Fn-bound wells (A) were incubated with 2 μg of rabbit polyclonal antibody against Fn. Binding of the polyclonal antibody (A) or mAb (C) was detected by incubating the wells with HRP-conjugated goat anti-(rabbit IgG) or secondary antibody [HRP-conjugated rabbit anti-(mouse IgG)], respectively. (B, D) Western blot. Purified amounts (8 μg) of full-length FnBRA and FnBRA lacking FnBPA-9 and FnBPA-10 (FnBRAΔ9,10) were separated on a 12.5% polyacrylamide gel and then electroblotted onto nitrocellulose membranes. The membranes were incubated with 10 μg of Fn or 10 μg of 15E11. Membranes incubated with Fn (B) were washed and further incubated with rabbit polyclonal antibody against Fn. Binding of the polyclonal antibody (B) or the mAb (D) to the filters was visualized with HRP-conjugated goat anti-(rabbit IgG) or rabbit anti-(mouse IgG), respectively.

of 15E11 and then tested for attachment to Fn-coated microtiter wells. Nonadherent bacteria were removed by washing, and the bound cells were detected with rabbit antibody against *S. aureus*. Under these conditions, 15E11 blocked adherence to Fn in a concentration-dependent fashion, with a maximal blocking effect at ~ 0.3 μM. Conversely, no inhibition was observed when bacteria were incubated with 14G6 (Fig. 9).

Discussion

The results presented in this study show that the FnBRs of FnBPB bound to Fn with different affinities. In fact, newly defined FnBRs (FnBPB-1, FnBPB-4, FnBPB-5, FnBPB-9, FnBPB-10, and FnBPB-11) bound Fn significantly better than the other repeats, and with K_D values in the nanomolar range. It was predicted from previous work [21] that binding affinities similar to that observed for the homologous repeats in FnBPA would be seen. Likewise, as FnBPB-1 is the first repeat and FnBPB-11 is the last, high-affinity Fn binding occurs over a large segment of FnBPB. The demonstration that FnBPB-1 binds Fn with high affinity is also important, as this indicates

Table 2. Kinetic and affinity parameters for 15E11–FnBR interactions. The parameters were determined by SPR measurements, with immobilized 15E11 as ligand and FnBRs of FnBPA and FnBPB as analytes. K_{on}, association rate constant; K_{off}, dissociation constant; K_D, dissociation equilibrium constant (means ± standard deviation, $n = 3$).

Protein	K_{on} ($M^{-1}\cdot s^{-1}$) (× 10^3)	K_{off} (s^{-1}) (× 10^{-4})	K_D (nM)
FnBPA-9	7.6 ± 0.8	2.9 ± 0.1	39.3
FnBPA-10	7.3 ± 0.8	3.3 ± 0.1	45.7
FnBPB-9	2.1 ± 0.2	4.3 ± 0.2	202.4
FnBPB-10	2.6 ± 0.2	3.7 ± 0.1	143.1

that the A-domain of FnBPB, which binds fibrinogen and elastin, and the first Fn-binding repeat are closer together than previously envisioned. This situation is again reminiscent of the A-region and FnBR organization of FnBPA [21]. Although not experimentally proven, it is most likely that the FnBRs from FnBPB interact with Fn at the NTD according to the β-zipper model.

We previously analyzed antibody reactivity to FnBPA in blood plasma from patients with staphylococcal infections. All patients had elevated levels of antibodies against FnBP as compared with those of young children, who presumably had not been exposed to staphylococcal infections. The antibodies against FnBPA preferentially reacted with the LIBSs in the repetitive region of the adhesin. Additionally, none of the IgG preparations from the patients' plasma inhibited the binding of Fn to isolated recombinant FnBPA or to intact staphylococci [21,36]. A similar picture emerged when mAbs were raised in mice immunized with the full-length FnBR region of FnBPA (FnBRA) [21] or FnBPB (manuscript in preparation). When the whole panel of mAbs against FnBRs from FnBPA or FnBPB was examined for reactivity towards recombinant FnBR preparations from both proteins in the presence or absence of Fn (or the NTD), all of the mAbs showed strong anti-LIBS activity. However, these results do not rule out the possibility that the immune system of the host might generate antibodies inhibiting the interaction of Fn with the repeats of both staphylococcal adhesins.

To eliminate the influence of Fn binding on antibody development, Huesca *et al.*, [37] using synthetic peptide immunogens lacking the ability to bind Fn, generated polyclonal antibodies and mAbs that were effective as inhibitors of Fn binding to FnBPA. Peptides derived from FnBPA expressed on cowpea mosaic virus and potato virus were also shown to be immunogenic, and the resulting sera blocked adherence of *S. aureus* to solid-phase-immobilized Fn [38].

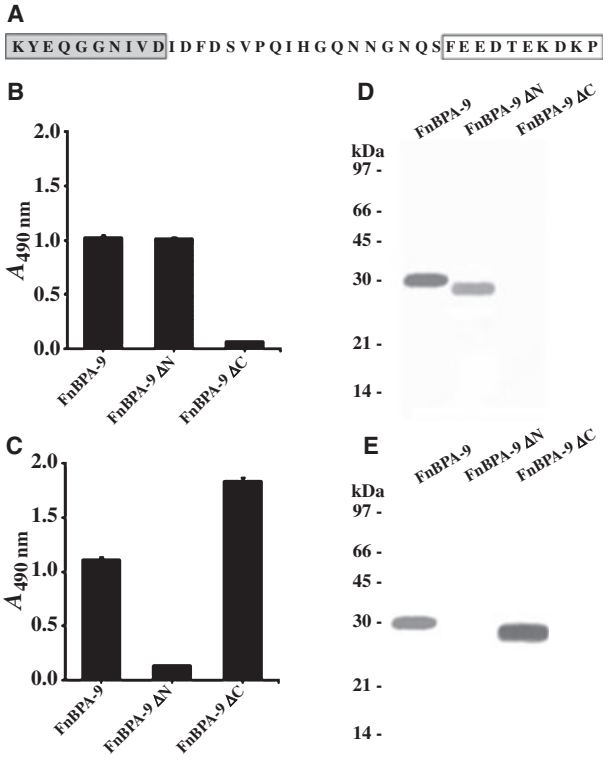

Fig. 7. Binding of Fn or 15E11 to FnBPA-9 lacking the N-terminal or C-terminal moieties. (A) Sequence of full-length FnBPA-9 and its deletion mutants. Amino acids deleted at the N-terminus and C-terminus are in gray and white boxes, respectively. (B, D) ELISA. Recombinant deletion mutants of FnBPA-9 lacking the first 10 N-terminal (FnBPA-9ΔN) or the last C-terminal (FnBPA-9ΔC) amino acids were immobilized on microtiter wells (1 μg in 100 μL) and probed with 100 μL of 20 $\mu g\cdot mL^{-1}$ Fn (B) or 100 μL of 10 $\mu g\cdot mL^{-1}$ 15E11 (D). After washing, the wells incubated with Fn were supplemented with 2 μg of rabbit polyclonal antibody against Fn. Bound antibody was detected by incubating the wells with secondary antibodies [HRP-conjugated goat anti-(rabbit IgG) (B) or rabbit anti-(mouse IgG) (D)]. (C, E) Western blot. Purified FnBPA-9ΔN and FnBPA-9ΔC (8 μg) were separated on 12.5% polyacrylamide gels and electroblotted onto nitrocellulose membranes. The membranes were incubated with 10 μg of Fn (C) or 10 μg of 15E11 (E). After washing, the membrane incubated with Fn (C) was incubated with rabbit polyclonal antibody against Fn. Binding of the polyclonal antibody (C) or mAb (E) to the filters was visualized by the addition of HRP-conjugated goat anti-(rabbit IgG) or rabbit anti-(mouse IgG), respectively.

Following this line of investigation, we isolated and characterized a mAb, named 15E11, from a hybridoma clone obtained by immunizing mice with the repetitive region of FnBPB. The mAb bound specifically and with high affinity to an epitope shared by repeats 9 and 10 from both FnBPA and FnBPB. Truncated forms of FnBPA-9 lacking 10 N-terminal or 10 C-terminal amino acids were tested by ELISA and western

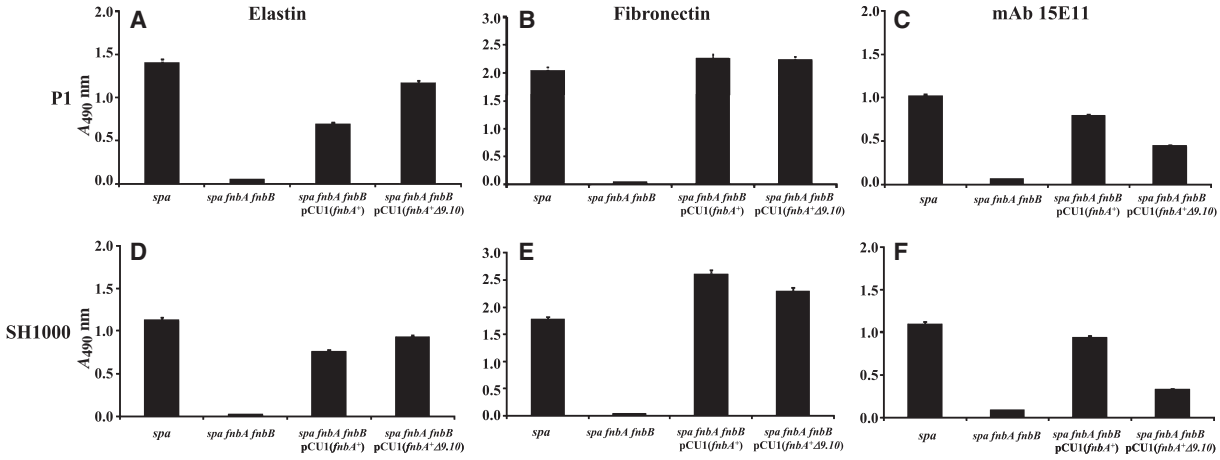

Fig. 8. 15E11 epitopes are displayed on the surface of *S. aureus* strains. Attachment of *S. aureus* to surface-coated elastin and Fn. Microtiter wells coated with 1 μg of elastin (A–D) or Fn (B–E) were incubated with 2.5×10^8 cells per mL of *S. aureus* strains P1 (A, B) and SH1000 (D, E). After several washings, 1 μg of rabbit polyclonal antibody against *S. aureus* was added. Bound antibody was detected by incubation with secondary antibody [HRP-conjugated goat anti-(rabbit IgG)]. (C, F) Binding of 15E11 to surface-coated *S. aureus* cells. Microtiter wells coated with 2.5×10^8 cells per mL *S. aureus* P1 (C) and SH1000 (F) were incubated with 1 μg of 15E11. Bound antibody was detected by incubation with secondary antibody [HRP-conjugated rabbit anti-(mouse IgG)].

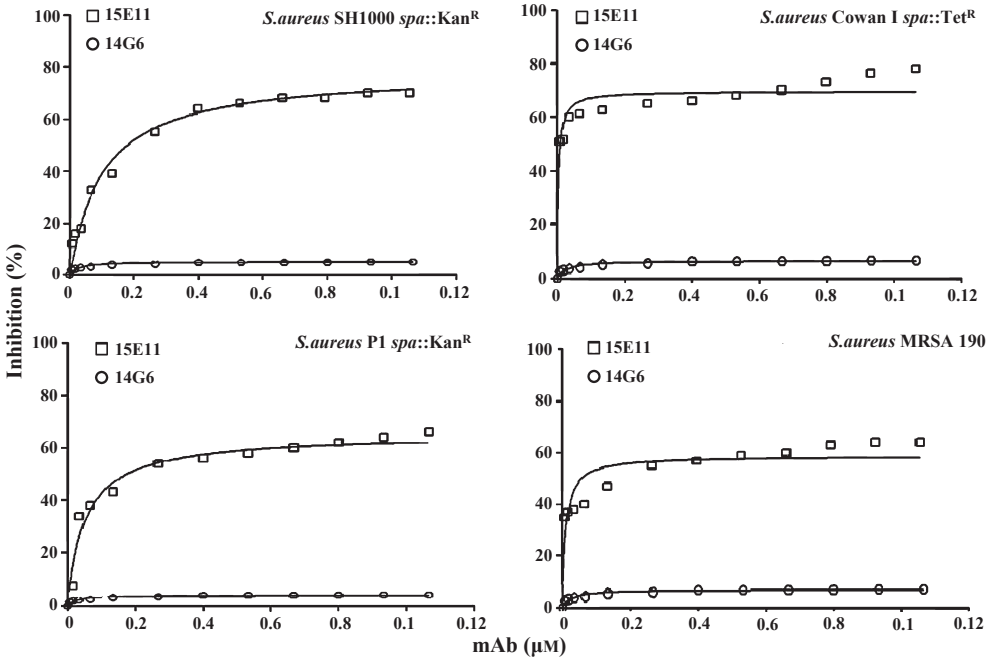

Fig. 9. Effect of 15E11 on the binding of *S. aureus* strains to surface-coated Fn. Microtiter wells were coated with 1 μg of Fn, and 2.5×10^7 cells of the indicated *S. aureus* strains preincubated with increasing amounts of mAbs 15E11 and 14G6 were added. After several washings, the wells were incubated with 0.5 μg of rabbit polyclonal antibody against *S. aureus*. Bound antibody was detected by incubation with secondary antibody [HRP-conjugated goat anti-(rabbit IgG)].

immunoblotting to map the epitope of 15E11. The mAb cannot bind to FnBPA-9 lacking the 10 N-terminal amino acids, whereas binding of Fn to FnBPA-9 was completely abolished when the C-terminal 10 amino acids were removed. Thus, Fn and 15E11 recognize distinct determinants in FnBPA-9. Alignment of repeats 9 and 10 of both FnBPA and FnBPB showed almost complete identity of their first 10 amino acids,

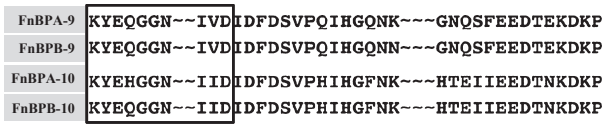

Fig. 10. Sequence alignment of repeats 9 and 10 from FnBPA and FnBPB. Segments including the first 10 amino acids in each repeat are boxed.

explaining the cross-reactivity of these repeats with 15E11, and suggesting the crucial role of the KYEQ(H)GGNIV(I)D sequence in epitope formation (Fig. 10). It is of note that the poor conservation of this stretch in the other repeat units of both adhesins is consistent with the marginal reactivity of the repeats to 15E11. Overall, these data confirm that the specific KYEQ(H)GGNIV(I)D sequence is the target of 15E11.

Solid-phase-binding assay, fluorescence microscopy and flow cytometry showed that the mAb epitope is clearly exposed on the surface of *S. aureus* cells. Consistent with this, the antibody blocked, in a dose-dependent fashion, attachment of staphylococci to immobilized Fn. However, the inhibitory activity of 15E11, although significant (70%), was incomplete, suggesting that the residual attachment of bacteria to Fn, even in the presence of excess amounts of 15E11, is mediated by repeats that are not targeted by the mAb. Interestingly, the inhibitory effect of 15E11 on the attachment of three distinct strains was substantially similar, suggesting that the epitopes are conserved and well exposed on the cell surface.

The finding that 15E11 is a blocking antibody, combined with the indication that Fn and the mAb map to different subsites on FnBPA-9, seems to suggest that the mechanism by which 15E11 inhibits ligand binding involves not merely competition with Fn, but also a conformational change in the repeat that results in preventing Fn from binding its own determinant. We refer to this phenomenon as 'the mAb-promoted conformational change mechanism'. A possible implication of this allosteric perturbation is that antibody binding shifts adhesin repeats from a high-affinity to a low-affinity state. As previously reported, the ligand-binding repeats of FnBPA [21], and possibly those of FnBPB in solution, have an intrinsically disordered structure in the apo-form. On binding to Fn, these motifs acquire conformations that can be monitored by specific mAbs recognizing LIBS epitopes [21] or by CD analysis [39]. Thus, the flexibility of the FnBPA-9 repeat fits well with the hypothesis of the mAb-promoted conformational change mechanism. Furthermore, it is noteworthy that repeat flexibility is the common prerequisite for both epitope binding by LIBS antibodies and the inhibitory activity of 15E11. Although the above mechanism could be strictly operational in the interaction of Fn with FnBPA-9, it is plausible that it is also effective in the binding of the ligand to the other repeats that share a common epitope. Other inhibition mechanisms cannot be excluded; among these, there is the possibility that, through the effect of the proximities of the antibody-binding and Fn-binding sites, the interaction of the repeat with Fn may be sterically hindered in the presence of the antibody.

The results of this study allow us to draw several conclusions. First, we confirm that the repeat region of FnBPB shows functional organization and immunological features of the homologous domain of FnBPA. Second, the epitopes recognized by 15E11 are localized to repeats 9 and 10 of both FnBPA and FnBPB, rather than being reactive with only a specific repeat. Third, although *S. aureus* adherence is mediated by several distinct repeats on both FnBPA and FnBPB, adhesion of bacteria to surface-coated Fn was inhibited significantly by the mAb, suggesting that the antibody-targeted repeats play a major role in Fn binding by FnBPA/FnBPB. Fourth, although a limited number of strains were tested, the antibody was an effective inhibitor of attachment to Fn, suggesting that a mAb with the ability to block all strains can be produced. Finally, the selection of a mAb that significantly reduces interaction of FnBPs with Fn indicates that the repetitive region of the major staphylococcal Fn-binding proteins, besides promoting the production of LIBS antibodies, has the potential to elicit the generation of blocking antibodies. Thus, the repetitive motifs of Fn-binding proteins from *S. aureus* could be successfully used as immunogens, and promote a blocking immune response by the host. This information leads to a reassessment of the value of the repetitive region of FnBPA/FnBPB as an immunogen, and raises the possibility of utilizing these proteins as components of a future anti-*S. aureus* vaccine.

Experimental procedures

Bacterial strains, plasmids, and culture conditions

The strains used are listed in Table 3 [23,40–45]. *Escherichia coli* strains were grown in LB broth or LB agar (Becton Dickinson, Buccinasco, Italy), and *S. aureus* strains were grown in Tryptic Soy Broth or Tryptic Soy agar (Becton Dickinson) at 37 °C in the presence of appropriate antibiotics with constant shaking.

Table 3. *S. aureus* and *E. coli* strains used in this work.

Strain	Relevant genotype	Properties	Source or reference
S. aureus			
8325-4	Wild type	NTCT 8325 cured of prophages; 11 bp deletion in *rsbU*	40
8325-4 *spa*	*spa*::Kanr	Mutant strain of 8325-4 defective in protein A	41
SH1000	Wild type	Strain 8325-4 with repaired defect in *rsbU*	42
SH1000 *spa*	*spa*::Kanr	Mutant strain of SH1000 defective in protein A	41
SH1000 *fnbA fnbB*	*fnbA*::Tetr *fnbB*::Ermr	Mutant strain of SH1000 defective in FnBPs	43
SH1000 *fnbA fnbB spa*	*spa*::Kanr *fnbA*::Tetr *fnbB*::Ermr	Mutant strain of SH1000 defective in FnBPs and protein A	This work
SH1000 *fnbA fnbB spa* (pCU1 *fnbA+*)	*spa*::Kanr *fnbA*::Tetr *fnbB*::Ermr (pCU1::*fnbA+* Cmr)	Mutant strain of SH1000 defective in FnBPs and protein A, complemented with plasmid expressing *fnbA+*	This work
SH1000 *fnbA fnbB spa* (pCU1 *fnbA+ D9,10*)	*spa*::Kanr *fnbA*::Tetr *fnbB*::Ermr (pCU1::*fnbA+* Δ9,10 Cmr)	Mutant strain of SH1000 defective in FnBPs and protein A, complemented with plasmid expressing *fnbA+* lacking repeats 9 and 10	This work
P1	Wild type	Rabbit virulent strain expressing FnBPs	44
P1 *spa*	*spa*::Kanr	Mutant strain of P1 defective in protein A	41
P1 *fnbA fnbB*	*fnbA*::Tetr *fnbB*::Ermr	Mutant strain of P1 defective in FnBPs	23
P1 *fnbA fnbB spa*	*spa*::Kanr *fnbA*::Tetr *fnbB*::Ermr	Mutant strain of P1 defective in FnBPs and protein A	This work
P1 *fnbA fnbB spa* (pCU1 *fnbA+*)	*spa*::Kanr *fnbA*::Tetr *fnbB*::Ermr (pCU1::*fnbA+* Cmr)	Mutant strain of P1 defective in FnBPs and protein A, complemented with plasmid expressing *fnbA+*	This work
P1 *fnbA fnbB spa* (pCU1 *fnbA+ D9,10*)	*spa*::Kanr *fnbA*::Tetr *fnbB*::Ermr (pCU1::*fnbA+* Δ9,10 Cmr)	Mutant strain of P1 defective in FnBPs and protein A, complemented with plasmid expressing *fnbA+* lacking repeats 9 and 10	This work
RN4220	*r-m+*	Restriction-negative 8325-4 derivative. Intermediate host for plasmid transfer from *E. coli* to *S. aureus*	45
Cowan I s*pa*	*spa*::Kanr	Mutant strain of Cowan defective in protein A	41
E. coli			
XL-1 Blue	*recA1 endA1* lac [F′ *proAB lac1q* Tn*10*(Tetr)]	Cloning host	Stratagene
BL21(DE3)	F– *ompT gal [dcm] [lon] hsdSB* (rB– mB–)	Cloning host	Novagen

Routine DNA manipulation and mutagenesis

DNA preparation, purification, restriction digestion, agarose gel electrophoresis and ligation were performed with standard methods [46] or following the manufacturer's instructions, unless otherwise stated. All enzymes were purchased from Roche Diagnostic (Milan, Italy). Plasmid DNA was isolated with the QIAprep Spin Miniprep kit (Qiagen, Monza, Italy). Routine preparation of *E. coli* competent cells and transformation of DNA into *E. coli* were performed by a one-step procedure [47]. Routine preparation of *S. aureus* electrocompetent cells and transformation of DNA into *S. aureus* were performed by electroporation.

The *spa*::Ka^R mutation was transduced from *S. aureus* strain 8325-4 *spa* into strains P1, P1 *fnbA fnbB*, SH1000 and SH1000 *fnbA fnbB* with phage-85 [48], selecting on 50 μg kanamycin mL^{-1}. The pCU1::$fnbA^+$ and pCU1::$fnbA^+$Δ9,10 constructs were transduced from strain RN4220 to strains P1 *fnbA fnbB spa* and SH1000 *fnbA fnbB spa* with phage-85 [48], selecting for resistance to 10 $\mu g \cdot mL^{-1}$ chloramphenicol.

Cloning of FnBR constructs

Cloning and expression of both the whole FnBRA and the recombinant individual repeats from FnBPA were performed as previously reported [21].

pQE30 and pET23b (GE Healthcare, Milan, Italy) were used as vectors for cloning and expression of FnBRA and and the whole FnBRB, respectively. pGEX-6P1 (GE Healthcare) was used as a vector for expressing the single repeats from both FnBPA and FnBPB.

A pBluescript vector encoding full-length *fnbB* was used as a template for all PCR reactions. In all cases, oligonucleotide primers were designed to encode *Bam*HI (5′-end) and *Eco*RI (3′-end) restriction sites (Table S1). PCR products

were digested with *Bam*HI and *Eco*RI, purified, and ligated to *Bam*HI-digested and *Eco*RI-digested pGEX-6p1 (for cloning all FnBRs) or pET-23b (for cloning FnBRB) (Table S1). The ligation mixtures were transformed into *E. coli* BL21(DE3), and the cells were incubated at 37 °C on LB agar plates (100 $\mu g \cdot mL^{-1}$ ampicillin) to select for transformants. Insertions were confirmed by DNA sequencing.

pQE30 and pET23b vectors harboring inserts corresponding to the repetitive regions of FnBPA and FnBPB, respectively, were used as templates for the inverse PCR reaction to produce the truncated forms of both proteins, lacking repeats 9 and 10.

The vector pGEX-5X carrying the insert for FnBPA-9 was used as a template for the PCR reaction to produce the truncates lacking the first 10 N terminal or the last 10 C-terminal amino acids of the repeat.

Expression and purification of recombinant FnBRs

FnBRs were expressed as GST fusion proteins. *E. coli* BL21(DE3) transformed with pGEX6P1 harboring the insert corresponding to each repeat was selected on LB agar (100 $\mu g \cdot mL^{-1}$ ampicillin). An overnight transformant culture was diluted 1 : 100 in LB medium and grown at 37 °C, with shaking, until the $D_{600\ nm}$ reached 0.5–0.6. Expression was induced by adding isopropyl-thio-β-D-galactoside (Inalco, Milan, Italy) to a final concentration of 0.3 mM. Bacteria were harvested by centrifugation at 1700 ***g*** for 5 min, and lysed by passage through a French press. The cell debris was removed by centrifugation (20 000 ***g***), and the filtered supernatant (0.45 μm membrane) was applied to a 5 mL glutathione–Sepharose-4B column (GE Healthcare). Fusion protein was eluted with five column volumes of 10 mM reduced glutathione (Sigma) in 50 mM Tris/HCl (pH 8.0). Fractions corresponding to the recombinant protein were pooled and extensively dialyzed against NaCl/P_i (140 mM NaCl, 2.7 mM KCl, 10.0 mM Na_2PO_4, 1.8 mM KH_2PO_4, pH 7.4). A single band of the expected molecular mass was observed for each of the different FnBR GST fusions when they were subjected to SDS/PAGE. Protein concentrations were determined with a bicinchoninic acid protein assay kit (Pierce, Rockford, IL, USA).

Preparation of Fn

Human Fn was prepared as previously reported [49,50]. For solid-phase-binding studies, the NTD was isolated with the procedure described by Zardi *et al.* [51].

Monoclonal antibody preparation

Monoclonal antibodies directed against FnBRB were raised with the procedure previously reported [52,53]. Isotyping of the mAbs was performed with a Mouse-Typer sub-isotyping kit (Zymed Laboratories, San Francisco, CA, USA). The hybridoma clone producing 15E11, an IgG_{2b-k}, was subcloned and grown to high cell density. The mAbs were purified from the supernatant by ammonium sulfate precipitation, followed by affinity chromatography on a protein G–Sepharose column, according to the manufacturer's protocol (GE Healthcare). Experiments with animals were carried out in accordance with the European Communities Council Directive of 24 November 1986 regarding the care and use of animals for experimental procedures.

Solid-phase-binding assays (ELISA)

Fn binding to FnBRA and FnBRB

Microtiter wells were coated for 1 h at 37 °C with 100 μL of 10 $\mu g \cdot mL^{-1}$ FnBPA-1, FnBPA-2, FnBPA-3, FnBPA-4, FnBPA-5, FnBPA-6, FnBPA-7, FnBPA-8, FnBPA-9, FnBPA-10, and FnBPA-11, and FnBPB-1, FnBPB-2/3, FnBPB-4, FnBPB-5, FnBPB-6, FnBPB-7, FnBPB-8, FnBPB-9, FnBPB-10, and FnBPB-11, in fusion with GST or with GST alone in coating buffer (50 mM sodium carbonate, pH 9.5). After washing with NaCl/P_i-T [NaCl/P_i containing 0.1% (v/v) Tween-20], the wells were blocked for 1 h at 22 °C with 200 μL of NaCl/P_i containing 2% (w/v) BSA. Subsequently, 100 μL of Fn (10 $\mu g \cdot mL^{-1}$) was added to the wells. Wells were washed with NaCl/P_i-T and incubated with 100 μL of a rabbit polyclonal antibody against human Fn (20 $\mu g \cdot mL^{-1}$) for 60 min. Binding of antibodies against Fn to the wells was detected by incubating the plates with horseradish peroxidase (HRP)-conjugated goat anti-(rabbit IgG) (1 : 1000 dilution; DakoCytomation, Glostrup, Denmark) for 45 min. The binding of the secondary antibody was quantified by adding the substrate *o*-phenylenediamine dihydrochloride and measuring the resulting absorbance at 490 nm in a microplate reader (Bio-Rad, Richmond, CA, USA).

Binding of 15E11 to FnBRs

Microtiter wells were coated for 1 h at 37 °C with the single recombinant repeats of FnBPA or FnBPB (10 $\mu g \cdot mL^{-1}$) in coating buffer (50 mM sodium carbonate, pH 9.5). After washing with NaCl/P_i-T, the wells were blocked for 1 h at 22 °C with 200 μL of NaCl/P_i containing 2% (w/v) BSA. Subsequently, 100 μL of the mAb (10 $\mu g \cdot mL^{-1}$) was added, and the wells were incubated for 1 h. Bound mAb was detected by incubating the wells with a 1 : 1000 dilution of HRP-conjugated rabbit anti-(mouse polyclonal IgG).

SDS/PAGE and western blotting

SDS/PAGE was performed with a 12.5% polyacrylamide gel. The gels were stained with Coomassie Brilliant Blue

(BioRad, Hercules, CA, USA). For the western blot assay, FnBRA, FnBRB and the corresponding single repeats were separated by SDS/PAGE, and then electroblotted onto a nitrocellulose membrane (GE Healthcare). The membrane was treated with a solution containing 5% dried milk in NaCl/P_i, washed, and incubated with 10 μg of Fn for 1 h at 22 °C. Following additional washings with NaCl/P_i, the membranes were incubated for 1 h with 2% milk in NaCl/P_i containing a rabbit polyclonal antibody against Fn. After several washings in NaCl/P_i-T (NaCl/P_i containing 0.5% Tween-20), the membranes were incubated for 45 min with 2% milk in NaCl/P_i including an HRP-conjugated goat anti-(rabbit IgG). Finally, the membranes were treated with ECL detection reagents 1 and 2 (GE Healthcare) according to the procedure recommended by the manufacturer, and exposed to an X-ray film for 10–20 s.

Effect of mAbs on staphylococcal attachment to surface-coated Fn

Microtiter wells were coated with 100 μL of 10 $\mu g \cdot mL^{-1}$ Fn. The remaining binding sites in the well were blocked by incubation with 200 μL of 2% BSA for 1 h at 22 °C. After washing with NaCl/P_i-T, the wells were incubated for 1 h at 22 °C with 2.5×10^7 cells of the indicated strains of *S. aureus* preincubated with increasing concentrations of 15E11 or the control mAb 14G6. After washing with NaCl/P_i-T, adherent cells were detected by incubation for 1 h with 100 μL (300 ng) of rabbit anti-(*S. aureus* polyclonal IgG). Binding of the antibody to bacteria was detected by incubating the plates with HRP-conjugated goat anti-(rabbit IgG) (1 : 1000 dilution; DakoCytomation, Glostrup, Denmark) for 45 min. The binding of the secondary antibody was quantified by adding the substrate *o*-phenylenediamine dihydrochloride and measuring the resulting absorbance at 490 nm in a microplate reader.

SPR analysis

SPR analysis of NTD binding to repeats was performed with the BIAcore X100 system (GE Healthcare). Goat antibody against GST (30 $\mu g \cdot mL^{-1}$; GE Healthcare) was diluted in 10 mM sodium acetate buffer at pH 5.0 and immobilized on CM5 sensor chips by amine coupling. This was performed with 1-ethyl-3-(3-dimethyl-aminopropyl) carbodiimide hydrochloride, followed by *N*-hydroxysuccinimide and ethanolamine hydrochloride, as described by the manufacturer. A single repeat fused to GST (2 $\mu g \cdot mL^{-1}$) was passed over the anti-GST surface of one flow cell while recombinant GST (5 $\mu g \cdot mL^{-1}$) was passed over the other flow cell to provide a reference surface. Increasing concentrations of the NTD were passed over the surface at a rate of 5 $\mu L \cdot min^{-1}$. All sensorgram data presented were subtracted from the corresponding data from the reference flow cell. The response generated from injection of buffer over the chip was also subtracted from all sensorgrams. Data were analyzed with BIAevaluation software version 3.0. A plot of the level of binding [resonance units (RU)] at equilibrium against concentration of analyte was used to determine the K_D.

Monoclonal antibody binding studies were carried out using the ProteOn XPR36 Protein Interaction Array system (Bio-Rad), based on SPR technology.

The 15E11 and 14G6 mAbs were covalently immobilized on parallel-flow channel surfaces of a Proteon GLC sensor chip (Bio-Rad), using amine coupling chemistry. This was performed by activating the surface for 5 min with a mixture of 1-ethyl-3-(3-dimethylaminopropyl)-carbodiimide (0.2 M) and sulfo-NHS (0.05 M), and then injecting the ligand (30 $\mu g \cdot mL^{-1}$ in sodium acetate, pH 5.0 for the antibodies and pH 4.0 for Fn), at a flow rate of 30 $\mu L \cdot min^{-1}$. The remaining activated groups were blocked with a 5 min injection of 1 M ethanolamine. The amount of ligand covalently immobilized on the surface, expressed in RU (1 RU = 1 pg protein per mm^2), was about 5000 RU. In parallel, a reference channel was prepared by using the same activation/deactivation procedure and injecting vehicle only. After the immobilization procedure, the fluidic system of ProteOn was rotated by 90°, allowing the testing in parallel of up to six different analytes, or up to six different concentrations of the same analyte, over the target surface.

Concentrations, ranging from 100 to 1000 nM, of each analyte were then injected over the immobilized ligand (or over the reference surface in parallel) at a rate of 30 $\mu L \cdot min^{-1}$ for 3 min (association phase). The dissociation phase was evaluated during the following 10 min. The vehicle was always injected in parallel-flow channels. The running buffer, NaCl/P_i (pH 7.4, 0.005% Tween-20; Biorad) was also used to dilute the analyte. All of the assays were performed at 25 °C.

The sensorgrams (time course of the SPR signal in RU) were normalized to a baseline value of 0. All sensorgram data presented were subtracted from the corresponding data obtained from the reference flow cell. The sensorgrams were fitted for the simplest 1 : 1 interaction model (Langmuir model; analysis software from Proteon, Columbus, OH, USA) to obtain the association and dissociation rate constants (K_{on} and K_{off}) and the corresponding equilibrium dissociation constant ($K_D = K_{off}/K_{on}$).

Fluorescence microscopy

Samples were observed with an Olympus BX51 microscope with standard fluorescence equipment. Blue excitation was performed with BP 450–480, DM 500 and barrier filter BA 515. Objectives UVPlanFl ×20 (0.50), UVPlanFl ×40 (0.75) and Plan ×40 (0.65) Ph were routinely used. The UPC-D condenser allowed the bright as well as the contrast field phase setting. Fluorescence microphotographs were taken using an Olympus Camedia C4040 digital camera.

Flow cytometry

Bacteria (2.5×10^8 cells) from the exponential phase ($D_{490\ nm}$ of ~ 0.6) were washed two times in NaCl/P_i, filtered (0.2 μm membrane), and then incubated in NaCl/P_i containing 300 μg of 15E11 or 14G6 for 1 h at 4 °C with moderate shaking.

Bacteria were harvested by centrifugation at 18 300 ***g*** for 5 min. The resulting pellet was resuspended in 500 μL of NaCl/P_i containing secondary antibody [FITC-conjugated goat anti-(mouse IgG)] at a 1 : 50 dilution for 1 h at 4 °C with moderate shaking. Samples were analyzed by a PAS II flow cytometer (Partec GmbH, Münster, Germany) equipped with an argon ion laser with 20 mW output power at 488 nm. Green fluorescence emission from FITC was measured in the FL1 channel (510–535 nm bandpass filter). Data were recorded and analyzed with FLOWMAX software from Partec.

Statistical analysis of ELISA experiments

Each experiment was repeated at least twice, with duplicate or triplicate measurements for every data point. Results are represented on graphs as the average of replicates in each experiment, with standard deviation used for error bars.

Acknowledgements

This work was supported by Fondazione CARIPLO 'Vaccines 2009-3546′ to P. Speziale and by a grant from Science Foundation Ireland to T. J. Foster.

References

1 Murakawa GJ (2004) Common pathogens and differential diagnosisof skin and soft tissue infections. *Cutis* **73**(Suppl), 7–10.
2 Cogen AL, Nizet V & Gallo RL (2008) Skin microbiota. A source of disease as defence? *Br J Dermatol* **158**, 442–455.
3 Lowy FD (1998) *Staphylococcus aureus* infections. *N Engl J Med* **339**, 520–532.
4 Valdvogel FA (1995) *Staphylococcus aureus* (including toxic shock syndrome). In *Principles and Practice of Infectious Diseases*, 4th edn (Mandel GL, Bennett JE & Dolin R eds), pp. 1754–1777. Churchill Livingstone, New York.
5 Sheagren JN (1984) *Staphylococcus aureus*. The persistent pathogen (Second of two parts). *N Engl J Med* **310**, 1437–1442.
6 Sherwood M, Smith D, Crisel R, Veledar E & Lerakis A (2006) Staphylococcus aureus endocarditis. The Grady Memorial hospital experienc. *J Med Sci* **331**, 84–87.
7 Ing MB, Baddour LM & Bayer AS (1997) Bacteremia and infective endocarditis: Pathogenesis, diagnosis and complications. In *The Staphylococci in Human Disease* (Crossley KB & Archer GL eds), pp. 331–354. Livingstone, New York.
8 Rupp ME (1997) Infections of intravascular catheters and vascular devices. In *The Staphylococci in Human Disease* (Crossley KB & Archer GL eds), pp. 379–399. Churchill Livingstone, New York.
9 Chambers HF & Deleo FR (2009) Waves of resistance: *Staphylococcus aureus* in the antibiotic era. *Nat Rev Microbiol* **7**, 629–641.
10 DeLeo FR & Chambers HF (2009) Reemergence of antibiotic-resistant *Staphylococcus aureus* in the genomic era. *J Clin Invest* **119**, 2464–2474.
11 Foster TJ (2009) Colonization and infection of the human host by staphylococci: adhesion, survival and immune evasion. *Vet Dermatol* **20**, 456–470.
12 Speziale P, Pietrocola G, Rindi S, Provenzano M, Provenza G, Di Poto A, Visai L & Arciola CR (2009) Structural and functional role of *Staphylococcus aureus* surface components recognizing adhesive matrix molecules of the host. *Future Microbiol* **4**, 1337–1352.
13 Hynes RO (1990) *Fibronectins*. *Springer Series in Molecular Biology*. Springer-Verlag, New York.
14 Wilson CJ, Clegg RE, Leavesley DI & Pearcy MJ (2005) Mediation of biomaterial–cell interactions by adsorbed proteins: a review. *Tissue Eng* **11**, 1–18.
15 Joh HJ, House-Pompeo K, Patti JM, Gurusiddappa S & Höök M (1994) Fibronectin receptors from gram-positive bacteria: comparison of active sites. *Biochemistry* **33**, 6086–6092.
16 Sottile J, Schwarzbauer J, Selegue J & Mosher DF (1991) Five type I modules of fibronectin form a functional unit that binds to fibroblasts and *Staphylococcus aureus*. *J Biol Chem* **266**, 12840–12843.
17 Talay SR, Zock A, Rohde M, Molinari G, Oggioni M, Pozzi G, Guzman CA & Chhatwal GS (2000) Co-operative binding of human fibronectin to SfbI protein triggers streptococcal invasion into respiratory epithelial cells. *Cell Microbiol* **2**, 521–535.
18 Raibaud S, Schwarz-Linek U, Kim JH, Jenkins HT, Baines ER, Gurusiddappa S, Höök M & Potts JR (2005) *Borrelia burgdorferi* binds fibronectin through a tandem beta-zipper, a common mechanism of fibronectin binding in staphylococci, streptococci and spirochetes. *J Biol Chem* **280**, 18803–18809.
19 Clarke SR, Harris LG, Richards RG & Foster SJ (2002) Analysis of Ebh, a 1.1-megadalton cell wall-associated fibronectin-binding protein of *Staphylococcus aureus*. *Infect Immun* **70**, 6680–6687.
20 Hussain M, Becker K, von Eiff C, Schrenzel J, Peters G & Herrmann M (2001) Identification and characterization of a novel 38.5-kilodalton cell surface protein of

Staphylococcus aureus with extended-spectrum binding activity for extracellular matrix and plasma proteins. *J Bacteriol* **183**, 6778–6786.
21 Meenan NA, Visai L, Valtulina V, Schwarz-Linek U, Norris NC, Gurusiddappa S, Höök M, Speziale P & Potts JR (2007) The tandem beta-zipper model defines high affinity fibronectin-binding protein within *Staphylococcus aureus* FnBPA. *J Biol Chem* **282**, 25893–25902.
22 Wann ER, Gurusiddappa S & Höök M (2000) The fibronectin-binding MSCRAMM FnbpA of *Staphylococcus aureus* is a bifunctional protein that also binds to fibrinogen. *J Biol Chem* **275**, 13863–13871.
23 Roche FM, Downer R, Keane F, Speziale P, Park PW & Foster TJ (2004) The N-terminal A domain of fibronectin-binding proteins A and B promotes adhesion of *Staphylococcus aureus* to elastin. *J Biol Chem* **279**, 38433–38440.
24 Schwarz-Linek U, Werner JM, Pickford AR, Gurusiddappa S, Kim JH, Pilka ES, Briggs JA, Gough TS, Höök M, Campbell ID *et al.* (2003) Pathogenic bacteria attach to human fibronectin through a tandem beta-zipper. *Nature* **423**, 177–181.
25 Bingham RJ, Rudiño-Piñera E, Meenan NA, Schwarz-Linek U, Turkenburg JP, Höök M, Garman EF & Potts JR (2008) Crystal structures of fibronectin-binding sites from *Staphylococcus aureus* FnBPA in complex with fibronectin domains. *Proc Natl Acad Sci USA* **105**, 12254–12258.
26 Jönsson K, Signas C, Muller HP & Lindberg M (1991) Two different genes encode fibronectin-binding proteins in *Staphylococcus aureus*. The complete nucleotide sequence and characterization of the second gene. *Eur J Biochem* **202**, 1041–1048.
27 Nashev D, Toshkova K, Salasia SI, Hassan AA, Lämmler C & Zschöck M (2004) Distribution of virulence genes of *Staphylococcus aureus* isolates from stable nasal carriers. *FEMS Microbiol Lett* **233**, 45–52.
28 Peacock SJ, Day NP, Thomas MG, Berendt AR & Foster TJ (2000) Clinical isolates of *Staphylococcus aureus* exhibit diversity in *fnb* genes and adhesion to human fibronectin. *J Infect* **41**, 23–31.
29 Arrecubieta C, Asai T, Bayern M, Loughman A, Fitzgerald JR, Shelton CE, Baron HM, Dang NC, Deng MC, Naka Y *et al.* (2006) The role of *Staphylococcus aureus* adhesions in the pathogenesis of ventricular assist device-related infections. *J Infect Dis* **193**, 1109–1119.
30 Fowler T, Johansson S, Wary KK & Höök M (2003) Scr kinase has a central role in in vitro cellular internalization of *Staphylococcus aureus*. *Cell Microbiol* **5**, 417–426.
31 Sinha B, Francois P, Que YA, Hussain M, Heilmann C, Moreillon P, Lew D, Krause KH, Peters G & Herrmann M (2000) Heterologously expressed *Staphylococcus aureus* fibronectin-binding proteins are sufficient for invasion of host cells. *Infect Immun* **68**, 6871–6878.
32 Sinha B, François PP, Nüsse O, Foti M, Hartford OM, Vaudaux P, Foster TJ, Lew DP, Herrmann M & Krause KH (1999) Fibronectin-binding protein acts as *Staphylococcus aureus* invasin via fibronectin bridging to integrin alpha5beta1. *Cell Microbiol* **1**, 101–117.
33 Peacock SJ, Foster TJ, Cameron BJ & Berendt AR (1999) Bacterial fibronectin-binding proteins and endothelial cell surface fibronectin mediate adherence of *Staphylococcus aureus* to resting human endothelial cells. *Microbiology* **145**, 3477–3486.
34 Heying R, van de Gevel J, Que YA, Moreillon P & Beekhuizen H (2007) Fibronectin-binding proteins and clumping factor A in *Staphylococcus aureus* experimental endocarditis: FnBPA is sufficient to activate human endothelial cells. *Thromb Haemost* **97**, 617–626.
35 Fitzgerald JR, Loughman A, Keane F, Brennan M, Knobel M, Higgins J, Visai L, Speziale P, Cox D & Foster TJ (2006) Fibronectin-binding proteins of *Staphylococcus aureus* mediate activation of human platelets via fibrinogen and fibronectin bridges to integrin GPIIb/IIIa and IgG binding to the Fc gammaRIIa receptor. *Mol Microbiol* **59**, 212–230.
36 Casolini F, Visai L, Joh D, Conaldi PG, Toniolo A, Höök M & Speziale P (1998) Antibody response to fibronectin-binding adhesin FnbpA from *Staphylococcus aureus* infections. *Infect Immun* **66**, 5433–5442.
37 Huesca M, Sun Q, Peralta R, Shivji GM, Sauder DN & McGavin MJ (2000) Synthetic peptide immunogens elicit polyclonal and monoclonal antibodies specific for linear epitopes in the D motifs of *Staphylococcus aureus* fibronectin-binding protein, which are composed of amino acids that are essential for fibronectin binding. *Infect Immun* **68**, 1156–1163.
38 Brennan FR, Jones TD, Longstaff M, Chapman S, Bellaby T, Smith H, Xu F, Hamilton WD & Flock JI (1999) Immunogenicity of peptides derived from a fibronectin-binding protein of *S. aureus* expressed on two different plant viruses. *Vaccine* **17**, 1846–1857.
39 House-Pompeo K, Xu Y, Joh D, Speziale P & Höök M (1996) Conformational changes in the fibronectin-binding MSCRAMMs are induced by ligand binding. *J Biol Chem* **271**, 1379–1384.
40 Novick R (1967) Properties of a cryptic high-frequency transducing phage in *Staphylococcus aureus*. *Virology* **33**, 155–166.
41 Patel AH, Foster TJ & Pattee PA (1989) Physical and genetic mapping of the protein A gene in the chromosome of *Staphylococcus aureus* 8325-4. *J Gen Microbiol* **135**, 1799–1807.
42 Horsburgh MJ, Aish JL, White IJ, Shaw L, Lithgow JK & Foster SJ (2002) sigmaB modulates determinant expression and stress resistance: characterization of a

functional rsbU strain derived from *Staphylococcus aureus* 8325-4. *J Bacteriol* **184**, 5457–5467.
43 Greene C, McDevitt D, Francois P, Vaudaux PE, Lew DP & Foster TJ (1995) Adhesion properties of mutants of *Staphylococcus aureus* defective in fibronectin-binding proteins and studies on the expression of *fnb* genes. *Mol Microbiol* **17**, 1143–1152.
44 Sherertz RJ, Carruth WA, Hampton AA, Byron MP & Solomon DD (1993) Efficacy of antibiotic-coated catheters in preventing subcutaneous *Staphylococcus aureus* infection in rabbit. *J Infect Dis* **167**, 98–106.
45 Kreiswirth BN, Löfdahl S, Betley MJ, O'Reilly M, Schlievert PM, Bergdoll MS & Novick RP (1983) The toxic shock syndrome exotoxin structural gene is not detectably transmitted by a prophage. *Nature* **305**, 709–712.
46 Sambrook J, Fritsch EF & Maniatis T (1989) *Molecular Cloning: a Laboratory Manual*, 2nd edn. Cold Spring Harbor Laboratory Press, Cold Spring Harbor, NY.
47 Chung CT, Niemela SL & Miller RH (1989) One step preparation of competent Escherichia coli: transformation and storage of bacterial cells in the same solution. *Proc Natl Acad Sci USA* **86**, 2172–2175.
48 Foster TJ (1998) Molecular genetic analysis of staphylococcal virulence. *Methods Microbiol* **27**, 433–454.
49 Vuento M & Vaheri A (1979) Purification of fibronectin from human plasma by affinity chromatography under non-denaturating conditions. *Biochem J* **183**, 331–337.
50 Speziale P, Visai L, Rindi S & Di Poto A (2008) Purification of human fibronectin using immobilized gelatin and Arg affinity chromatography. *Nat Protoc* **3**, 525–533.
51 Zardi L, Carnemolla B, Balza E, Borsi L, Castellani P, Rocco M & Siri A (1985) Elution of fibronectin proteolytic fragments from a hydroxyapatite chromatography column. A simple procedure for the preparation of fibronectin domains. *Eur J Biochem* **146**, 571–579.
52 Köhler G & Milstein C (1975) Continuous cultures of fused cells secreting antibody of predefined specificity. *Nature* **256**, 495–497.
53 Visai L, De Rossi E, Valtulina V, Casolini F, Rindi S, Guglierame P, Pietrocola G, Bellotti V, Riccardi G & Speziale P (2003) Identification and characterization of a new ligand-binding site in FnbB, a fibronectin-binding adhesin from *Streptococcus dysgalactiae*. *Biochim Biophys Acta* **1646**, 173–183.

Supporting information

The following supplementary material is available:
Fig. S1. SDS/PAGE of FnBRB, FnBRA and the relevant, predicted FnBRs.
Table S1. Oligonucleotide primers used for FnBRB, FnBPB repeats, and FnBRBΔ9,10, FnBPAΔ9,10 and FnBRAΔ9,10 constructs.

This supplementary material can be found in the online version of this article.

Please note: As a service to our authors and readers, this journal provides supporting information supplied by the authors. Such materials are peer-reviewed and may be re-organized for online delivery, but are not copy-edited or typeset. Technical support issues arising from supporting information (other than missing files) should be addressed to the authors.